

# Fast Iterative Configuration of Reconfigurable Intelligent Surfaces in mmWave Systems

Anna V. Guglielmi<sup>1</sup> and Stefano Tomasin<sup>1,2</sup>

<sup>1</sup> Dept. of Information Engineering, University of Padova, Italy

<sup>2</sup> Consorzio Nazionale Interuniversitario di Telecomunicazioni, CNIT, Parma, Italy  
email: {annavaleria.guglielmi, stefano.tomasin}@unipd.it

**Abstract**—Reconfigurable intelligent surfaces (RISs) are a promising solution to improve the coverage of cellular networks, thanks to their ability to steer impinging signals in desired directions. However, they introduce an overhead in the communication process since the optimal configuration of a RIS depends on the channels to and from the RIS, which must be estimated. In this paper, we propose a novel fast iterative configuration (FIC) protocol to determine the optimal RIS configuration that exploits the small number of paths of millimetre-wave (mmWave) channels and an adaptive choice of the explored RIS configurations. In particular, we split the elements of the RIS into a number of subsets equal to the number of channel taps. For each subset, then an iterative procedure finds at each iteration the optimal RIS configuration in a codebook exploring a two-dimensional grid of possible angles of arrival and departure of the path at the RIS. Over the iterations, the grid is made finer around the point identified in previous iterations. Numerical results obtained using an urban channel model confirm that the proposed solution is fast and provides a configuration close to the optimal in a shorter time than other existing approaches.

**Index Terms**—Reconfigurable intelligent surfaces (RISs), channel estimation, beamforming.

## I. INTRODUCTION

Reconfigurable intelligent surfaces (RISs) are seen as a key enabling technology for beyond fifth generation (B5G) wireless systems, due to their ability to purposely shape wireless environments [1]. An important challenge lies in the optimization of the phase-shifts, since beam management in millimetre-wave (mmWave) communications is a key technique to overcome the severe free-space path loss and atmospheric absorption [2], [3]. However, two main difficulties arise in RIS optimization: (i) the problem is non-convex, due to the unit modulus constraint; (ii) the impact of phase shifts on performance metrics such as the signal-to-noise ratio (SNR) or the achievable rate is typically coupled with other unknown system model parameters.

The majority of the existing works aim at optimizing the RIS elements individually for real-time communications, leading to computationally expensive solutions when the number

of elements is large. It has been shown that for usual outdoor scenarios, hundreds or even thousands of RIS elements are needed to generate a virtual line-of-sight (LoS) link as strong as a LoS [4]. Thus, most algorithms in the literature are not suitable for large RISs: due to their complexity, several solutions have been considered. To overcome this problem, the design of a codebook of phase-shift configurations in an offline fashion is proposed in [4], followed by the selection of the best codeword from the set in an online optimization fashion for the given channel realization. In [5], [6], predefined phase-shift configurations based on the discrete Fourier transform (DFT) matrix for channel estimation in a RIS-assisted system are employed. Nevertheless, DFT-based codebooks consist of the same number of phase-shift configurations as the number of RIS elements, which are too many for practical implementation. Consequently, in [7] a quadratic codebook design is proposed, featuring a parameter for the control of the codebook size. It has been shown that under the far-field assumption, the overhead of beam training with exhaustive search can be significantly reduced using small-size RIS phase shifts codebooks. A variable-width hierarchical phase-shift codebook suitable for both the near- and far-field of the RIS in mmWave communication systems was proposed in [8]. Instead, [4]–[8] focus on continuous RIS phase shifts; however, discrete RIS phase shifts are to be preferred to reduce the implementation cost at the expense of increasing the complexity of the optimization problem. Recently, in [9], [10] a generic framework has been proposed, aiming at optimizing the end-to-end precoder controlled by RISs so that arbitrary beam patterns can be generated, given a predefined lookup table of RIS element-wise complex reflection coefficients. In [11] the RIS optimization is framed as two offline optimization problems towards a favorable trade-off between power consumption and codebook size. However, in [9]–[13], the RIS configuration optimization is based on the knowledge of the channels to and from I, which is not easily obtainable.

Alternative methods have been proposed to mitigate the overhead due to cascade channel estimation and reduce the delay introduced by the RIS optimization, including beam training and exploiting the RIS diversity gain [14]–[16]. Nevertheless, again obtaining an accurate knowledge of the underlying channel is quite challenging: even when the channel model is linear and known, the imprecise knowledge of the parameters of the channel, can significantly degrade the performance. To

Project funded under the National Recovery and Resilience Plan (NRRP), Mission 4 Component 2 Investment 1.3 - Call for tender No. 341 of 15 mar 2022 of Italian Ministry of University and Research funded by the European Union - NextGenerationEU Project code MUR: PE\_0000001 Concession Decree No. 1549 of 11/10/2022 adopted by the Italian Ministry of University and Research, CUP C93C22005250001 Project title REsearch and innovation on future Telecommunications systems and networks, to make Italy more smART (RESTART)

overcome this problem, the optimization can be done before channel estimation. However, only a few works address it and employ approaches such as maximizing recovery performance by means of DFT or Hadamard matrices, or exploiting external location information [17], [18], which however may not be accurate enough and becomes problematic in the presence of non-line-of-sight (NLOS) propagation conditions.

In this paper, we propose the novel fast iterative configuration (FIC) algorithm that configures the RIS elements for the uplink of a cellular system operating at mmWave frequencies. We assume that the channels are unknown and we leverage the fact that at those frequencies the number of channel paths is very small. We also exploit the fact that the receiving base station (which can estimate the channel) is also controlling the RIS. Thus, we propose an adaptive iterative algorithm. FIC first partitions the RIS elements into subsets, where each subset is configured to reflect one path. For each subset, we apply an iterative algorithm, where at each iteration the source-RIS-destination channel is estimated for a set of RIS configurations, and the resulting achievable rate is computed. Each RIS configuration is associated with a couple of angle of arrival (AoA) and angle of departure (AoD) at the RIS, and the angles of the set are on a regularly-spaced two-dimensional (2D) angle grid. The configuration providing the highest achievable rate is selected and its AoD-AoA couple becomes the center of a second smaller and finer grid for the next iteration. The configuration of the RIS for a given channel realization is thus iteratively adjusted towards the maximization of the achievable rate. It is worth noting that the proposed approach does not assume the complete knowledge of the channels from and to the RIS, and considers discrete phase-shift values.

The rest of the paper is organized as follows. Section II describes the system model. Section III describes the FIC algorithm and the design of the explored RIS configurations. Numerical results are presented and discussed in Section IV. Lastly, Section V concludes the paper.

## II. SYSTEM MODEL

We consider a narrowband single-user multiple-input multiple-output (MIMO) mmWave communication system, wherein the transmission from a source (S) to a destination (D) is assisted by an RIS (I) as shown in Fig. 1. The RIS I is controlled by D, and, with reference to a cellular system, this model corresponds to an uplink transmission scenario, where S is the user equipment and D is the base station.

S and D are equipped with uniform linear arrays (ULAs) with  $N_S$  and  $N_D$  antennas, respectively. The RIS has  $N_I$  passive reflective elements equally spaced along a line. We assume that the direct S-D channel is blocked, while connectivity between S and D is maintained through I.

We denote with  $\mathbf{G} \in \mathbb{C}^{N_I \times N_S}$  and  $\mathbf{H} \in \mathbb{C}^{N_D \times N_I}$  the narrowband S-I and I-D channel matrices, respectively. We adopt a block-fading channel model, thus both  $\mathbf{G}$  and  $\mathbf{H}$  remain constant during the channel coherence time.

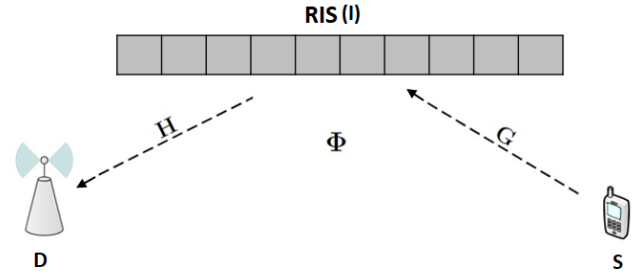


Figure 1. System model.

In the mmWave band, channels have only a few relevant paths, thus we can use a geometric model for their description. Let  $d$  be the spacing between both the RIS elements and the antennas at S and D; then, the array response column vector for an angle of arrival or departure  $\beta$  is

$$[\boldsymbol{\alpha}(\beta)]_n = e^{j2\pi \frac{d}{\lambda} (n-1) \sin \beta}, \quad n = 1, \dots, N_S. \quad (1)$$

For channel  $\mathbf{G}$ , let  $[\rho_G]_l$  be the  $l$ th propagation path gain,  $L_G$  be the number of paths, vectors  $\boldsymbol{\theta}_G \in [-\pi, \pi]$  and  $\boldsymbol{\eta}_G \in [-\frac{\pi}{2}, \frac{\pi}{2}]$  be the AoD and the AoA of the channel, respectively. Here, we assume that both S and D are on the same side of the RIS, while the antennas of D can have any orientation on the plane. By following the geometric channel model, channel  $\mathbf{G}$  with  $L_G$  paths can be written as

$$\mathbf{G} = \sum_{l=1}^{L_G} [\rho_G]_l \boldsymbol{\alpha}([\boldsymbol{\eta}_G]_l) \boldsymbol{\alpha}^H([\boldsymbol{\theta}_G]_l) \quad (2)$$

$$= \mathbf{A}(\boldsymbol{\eta}_G) \text{diag}(\boldsymbol{\rho}_G) \mathbf{A}^H(\boldsymbol{\theta}_G), \quad (3)$$

where  $^H$  is the Hermitian operator and the array response matrices, i.e.,  $\mathbf{A}(\boldsymbol{\theta}_G)$  and  $\mathbf{A}(\boldsymbol{\eta}_G)$ , are defined as

$$\mathbf{A}(\boldsymbol{\theta}_G) = [\boldsymbol{\alpha}([\boldsymbol{\theta}_G]_1), \dots, \boldsymbol{\alpha}([\boldsymbol{\theta}_G]_{L_G})], \quad (4)$$

$$\mathbf{A}(\boldsymbol{\eta}_G) = [\boldsymbol{\alpha}([\boldsymbol{\eta}_G]_1), \dots, \boldsymbol{\alpha}([\boldsymbol{\eta}_G]_{L_G})]. \quad (5)$$

Similarly, channel  $\mathbf{H}$  is modeled as

$$\mathbf{H} = \sum_{l=1}^{L_H} [\rho_H]_l \boldsymbol{\alpha}([\boldsymbol{\eta}_H]_l) \boldsymbol{\alpha}^H([\boldsymbol{\theta}_H]_l), \quad (6)$$

$$= \mathbf{A}(\boldsymbol{\eta}_H) \text{diag}(\boldsymbol{\rho}_H) \mathbf{A}^H(\boldsymbol{\theta}_H), \quad (7)$$

where  $[\rho_H]_l$  is the  $l$ th propagation path gain,  $L_H$  is the number of paths,  $\boldsymbol{\theta}_H \in [-\frac{\pi}{2}, \frac{\pi}{2}]$  and  $\boldsymbol{\eta}_H \in [-\frac{2}{6}\pi, \frac{2}{6}\pi]$  are the AoD and the AoA of the channel, respectively. Here we assumed that the field of view of D is of  $30^\circ$ .

By applying (3) and (7), and considering the configuration of I, the complete end-to-end uplink channel between S and D is expressed as

$$\mathbf{Q} = \mathbf{H}\boldsymbol{\Phi}\mathbf{G}, \quad (8)$$

where  $\boldsymbol{\Phi} \in \mathbb{C}^{N_I \times N_I}$  is the phase control matrix at I with unit-modulus elements on the diagonal, i.e.,  $[\boldsymbol{\Phi}]_{k,k} = e^{j\phi_k}$ , with  $\phi_k \in [0, 2\pi)$  and  $k = 1, \dots, N_I$ .

### III. CHANNEL ESTIMATION PROTOCOL

Our aim is to optimize  $\Phi$  to maximize the resulting achievable rate

$$C(\mathbf{Q}) = \log_2 \det \left( \mathbf{I} + \frac{1}{\sigma^2} \mathbf{Q}^H \mathbf{Q} \right), \quad (9)$$

where  $\sigma^2$  is the noise power. We assume that channels  $\mathbf{H}$  and  $\mathbf{G}$  are not known to D. However, instead of first estimating the channels  $\mathbf{H}$  and  $\mathbf{G}$  (or, equivalently, the parameters  $\eta_H, \theta_H, \rho_H, \eta_G, \theta_G,$  and  $\rho_G$ ) and then maximize the achievable rate, we directly seek the optimal RIS configuration by an iterative adaptive procedure, denoted FIC, where we leverage the fact that D has the control of I, thus can choose the configuration to be explored according to the performance obtained from previous configurations.

In particular, first S transmits pilot signals that let D estimate the resulting channel  $\mathbf{Q}$  for a set of  $L_1$  configurations

$$\mathcal{S}_1 = \{\Phi_{1,1}, \dots, \Phi_{1,L_1}\}, \quad (10)$$

and the resulting uplink channel estimates are  $\hat{\mathbf{Q}}_{1,1}, \dots, \hat{\mathbf{Q}}_{1,L_1}$ . Based on these estimates, and on the computation of the resulting achievable rate  $C(\hat{\mathbf{Q}}_{1,\ell})$ ,  $\ell = 1, \dots, L_1$ , D selects a new set of configurations, then S transmits pilots and D obtains the channel estimates for the new configurations.

In general, at iteration  $i > 1$ , S transmits pilots in correspondence of  $L_i$  RIS configurations in the set

$$\mathcal{S}_i = \{\Phi_{i,1}, \dots, \Phi_{i,L_i}\}, \quad (11)$$

and the resulting channel estimates are  $\hat{\mathbf{Q}}_{i,1}, \dots, \hat{\mathbf{Q}}_{i,L_i}$ . D also computes the resulting achievable rate  $C(\hat{\mathbf{Q}}_{i,\ell})$ ,  $\ell = 1, \dots, L_i$ . The FIC algorithm is stopped when a maximum number  $I$  of iterations is reached. The choice of the configuration sets  $\mathcal{S}_i$  is detailed in the following.

The idea of the FIC algorithm is to progressively improve the precision of the selected configuration to maximize the resulting achievable rate. Moreover, we leverage the fact that mmWave channels are characterized by a small number of paths. Note that we do not explicitly estimate all the channel parameters, e.g., we do not estimate the angles at the devices and the channel gains.

We first describe the FIC algorithm when a single path is present ( $L_G = L_H$ ) and then we consider the general case with multiple paths.

#### A. RIS Configuration With A Single-Path Channel

First, we observe that for single-path channels ( $L_G = L_H = 1$ ), the RIS configuration maximizing the achievable rate aligns the steering vectors of the channels, i.e.,

$$\bar{\Phi} = \text{diag}\{e^{j\bar{\phi}_k}\} = \arg \max_{\Phi} \|\mathbf{A}^H(\theta_H)\Phi\mathbf{A}(\eta_G)\|^2, \quad (12)$$

where, for  $k = 1, \dots, N_I$ ,

$$\bar{\phi}_k = 2\pi \frac{d}{\lambda} (\sin \bar{\theta} - \sin \bar{\eta})(k-1), \quad (13)$$

with  $\bar{\theta} = \theta_H$  and  $\bar{\eta} = \eta_G$ . We recall that the AoA and AoD at the RIS are in the range  $[-\frac{\pi}{2}, \frac{\pi}{2}]$  with respect to the firing direction of the linear element array.

Therefore, we design the RIS configurations  $\Phi_{1,\ell}$  as in (12), with a suitable choice of the angles  $\bar{\theta}$  and  $\bar{\eta}$ .

At the first iteration ( $i = 1$ ) of the FIC algorithm, a regularly-spaced 2D grid of  $L_1$  angle couples is designed inside a square with side  $[-\frac{\pi}{2}, \frac{\pi}{2}]$ . In particular, the phases of the RIS configuration are  $[\Phi_{1,\ell}]_{k,k} = e^{j\phi_k^{(1,\ell)}}$ , with (for  $i = 1$  and  $\ell = 1, \dots, L_1$ )

$$\phi_k^{(1,\ell)} = 2\pi \frac{d}{\lambda} (\sin \theta^{(i,\ell)} - \sin \eta^{(i,\ell)})(k-1) \quad (14)$$

and

$$\theta^{(1,\ell)} = \frac{\pi}{\sqrt{L_1}} \left[ \left\lfloor \frac{\ell-1}{\sqrt{L_1}} \right\rfloor - \frac{\sqrt{L_1}}{2} \right] + \frac{\pi}{2\sqrt{L_1}}, \quad (15)$$

$$\eta^{(1,\ell)} = \frac{\pi}{\sqrt{L_1}} \left[ \text{mod}(\ell-1, \sqrt{L_1}) - \frac{\sqrt{L_1}}{2} \right] + \frac{\pi}{2\sqrt{L_1}}, \quad (16)$$

where  $\lfloor x \rfloor$  is the integer floor of  $x$ , and  $\text{mod}(x, L)$  is the remainder of  $x/L$ .

The index of the RIS configuration  $\bar{\Phi}^{(1)} = \Phi_{1,\bar{\ell}}$  providing the largest achievable rate is found as

$$\bar{\ell} = \arg \max_{\ell} C(\hat{\mathbf{Q}}_{1,\ell}) \quad (17)$$

and is used to design a new grid and start another iteration of the algorithm.

In general, at iteration  $i > 1$ , defining  $\gamma_i = \sqrt{\prod_{k=1}^i L_k}$ , the regularly-spaced 2D grid of  $L_i$  cells is designed inside a square with side  $\pi/\gamma_i$ , and the phases of the RIS configuration  $[\Phi_{i,\ell}]_{k,k} = e^{j\phi_k^{(i,\ell)}}$  are given by (14) and

$$\theta^{(i,\ell)} = \frac{\pi}{\gamma_i} \left[ \left\lfloor \frac{\ell-1}{\sqrt{L_i}} \right\rfloor - \frac{\sqrt{L_i}}{2} \right] + \frac{\pi}{2\gamma_i} + \bar{\theta}^{(i-1)}, \quad (18)$$

$$\eta^{(i,\ell)} = \frac{\pi}{\gamma_i} \left[ \text{mod}(\ell-1, \sqrt{L_i}) - \frac{\sqrt{L_i}}{2} \right] + \frac{\pi}{2\gamma_i} + \bar{\eta}^{(i-1)}, \quad (19)$$

where  $\bar{\theta}^{(i-1)}$  and  $\bar{\eta}^{(i-1)}$  are the angles of the RIS configuration  $\bar{\Phi}^{(i-1,\bar{\ell})}$  selected at the previous iteration with

$$\bar{\ell} = \arg \max_{\ell \in \{1, \dots, L_{i-1}\}} C(\hat{\mathbf{Q}}_{i-1,\ell}). \quad (20)$$

When  $i = I$ , the procedure stops providing the RIS configuration  $\bar{\Phi}^{(I,\bar{\ell})}$ .

*Multiple Starting Points:* The iterative procedure in general will find a local maximum of the achievable rate, as the achievable rate is not a convex function of the AoA and AoD. To improve the performance of FIC, multiple starting points can be considered. In this case,  $P$  RIS configurations are selected from those explored at the first iteration, and the iterative procedure is applied on all the  $P$  selected angle couples to find  $P$  local maxima. Then, the configuration yielding the maximum achievable rate is selected as the final solution. Note that this increases the duration of the FIC algorithm while bringing it closer to the optimal RIS configuration.

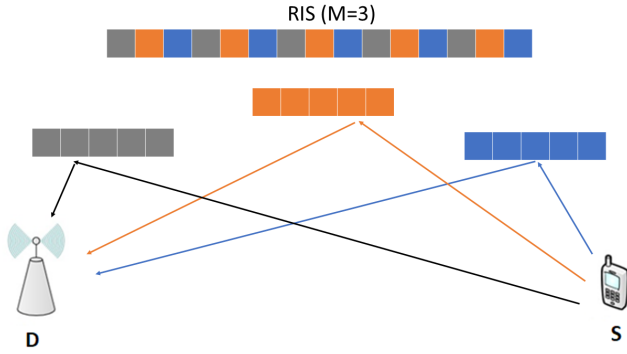


Figure 2. Example of multi-path scenario with  $M = 3$ .

### B. RIS Configuration With Multi-Path Channel

When multiple paths are present, we partition the RIS elements into  $M$  sets of  $N_I/M$  elements each, where set  $m$  will have phases aligned to the  $m$ -th path, between S and I with the  $m$ -th path between I and D. Since one AoA at the RIS will be matched to a single AoD from the RIS, we will consider  $M = \min\{L_G, L_H\}$  configurations, as shown in Fig. 2 for  $M = 3$ .

Therefore, we repeat the algorithm of Section III-A to find the configuration of the various RISs. Since RIS elements cannot be switched off, we propose the following procedure, operating in  $M$  steps, where in each step we select the configuration for  $N_I/M$  RIS elements.

In the first step, we configure all the  $N_I$  RIS elements using the iterative procedure of Section III-A. Then, we fix the obtained configuration for  $N_I/M$  elements, starting from the first and regularly spaced by  $M - 1$  elements.

In step  $m > 1$ , we optimize the

$$N_I - (m - 1) \frac{N_I}{M} \quad (21)$$

elements not yet fixed, and then we fix the obtained configuration for  $N_I/M$  elements, starting from the  $m$ -th and regularly spaced by  $M - 1$  elements. When configuring the set  $m$  of the RIS elements, we compute the achievable rate (9) by considering the already set values of the phases for the  $m - 1$  sets already optimized.

Note that we do not put additional constraints on the configuration selection procedure. Thus, it may happen that more than one RIS subset is configured for the same angles, thus serving the same path. This occurs when the achievable rate gain obtained by a stronger reflection is higher than that associated with the larger multiplexing provided by reflecting an additional path. Still, our algorithm performs this tradeoff implicitly, without the need for further elaboration.

Lastly, note that although the RIS configurations are tuned to specific AoAs and AoDs of the RIS, they also contribute to the reflection of other paths, thus each sub-block of the RIS is in practice not strictly associated to a single path but contributes to the whole resulting achievable rate in a more elaborate way.

### C. Estimation Time

Assuming that the number of pilot symbols for each RIS configuration is fixed and their transmission takes time  $T_0$ , the total time spent by the FIC algorithm is

$$T_{\text{FIC}} = T_0 M \left( L_1 + P \sum_{i=2}^I L_i \right), \quad (22)$$

since to configure each of the  $M$  sub-array of the RIS we need  $I$  iterations, each requiring the exploration of  $L_i$  RIS configurations. Moreover, we have taken into account the possibility of using  $P$  starting points.

## IV. NUMERICAL RESULTS

In this section, we assess the performance of the proposed FIC algorithm. We consider a single-user cellular uplink transmission system assisted by a RIS and an urban micro-cell (UMi) scenario for a mmWave transmission at the carrier frequency of 28 GHz, considering the geometry-based stochastic channel model used in 3GPP [19]. The SNR is set at  $-15$  dB.

We assume that both S-I and I-D links exhibit a LoS condition remarking that the direct link between S and D is blocked. S and D are equipped with an ULA array of  $N_S = 2$  and  $N_D = 4$  antennas, respectively. For the RIS, we consider  $N_I = 120$  elements along a line spaced  $d = \lambda/2$ , where  $\lambda$  is the wavelength at the carrier frequency. We assume  $T_0 = 1$ , thus  $T$  counts the number of channel estimates.

For comparison purposes, we consider a scheme wherein the channel is estimated for a set of RIS configurations and select the one providing the highest achievable rate. This corresponds to stopping the interactive procedure on the first iteration  $I = 1$  while considering denser grids (i.e., larger values of  $L_1$ ). This scheme is denoted by baseline (BAS) configuration.

Performance is evaluated in terms of the average normalized achievable rate loss (averaged over the channel and noise realizations)

$$\epsilon = \mathbb{E} \left[ \frac{C_{\text{opt}} - \hat{C}}{C_{\text{opt}}} \right], \quad (23)$$

where  $C_{\text{opt}}$  is the achievable rate obtained with the optimal RIS configuration, whereas  $\hat{C}$  is the achievable rate obtained with the RIS configuration of the FIC algorithm (or BAS). For multi-path channels,  $C_{\text{opt}}$  must be determined through an exhaustive search.

Figs. 3 and 4 show the average normalized achievable rate loss  $\epsilon$  as a function of the total number of channel estimates  $T$  for an element/antenna spacing  $d = \lambda/2$ . Two values of the number of channel paths are considered, namely,  $L_G = L_H = 2$  and  $L_G = L_H = 3$ , and for the choice of the configuration the RIS is split into  $M = 2$  and 3 sub-blocks, respectively. On the grid choice for FIC, we consider two cases: a)  $L_i$  is constant at all iterations, and b)  $L_i$  changes at the various iterations. In particular, for case a) we considered  $L_i = 9, 16, 25, 36$ , and 64, while for case b) we considered the following alternatives: 1)  $L_1 = 25$ ,  $L_i = 9$  for  $i > 1$ , 2)  $L_1 = 36$ ,  $L_i = 9$  for  $i > 1$ , and 3)  $L_1 = 64$ ,  $L_2 = 36$ ,  $L_i = 9$  for  $i > 2$ .

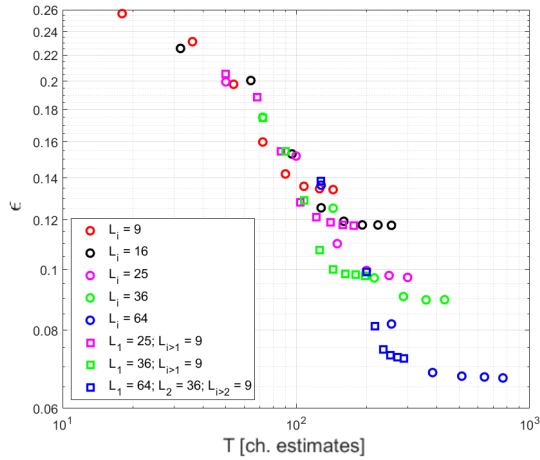


Figure 3. Average normalized achievable rate loss varying  $L_i$  with  $L_G = L_H = 2$  paths and element/antenna spacing  $d = \frac{\lambda}{2}$ .

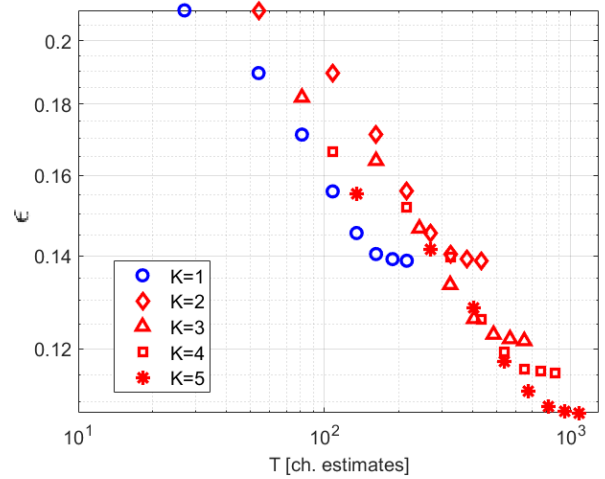


Figure 5. Average normalized achievable rate loss varying the number of channel estimates per iteration  $K = 1, 2, 3, 4,$  and  $5$  with  $L_i = 9$   $L_G = L_H = 3$  paths and element/antenna spacing  $d = \frac{\lambda}{2}$ .

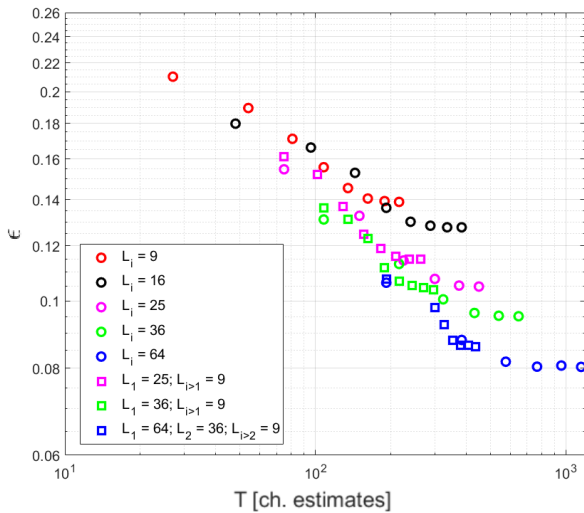


Figure 4. Average normalized achievable rate loss varying  $L_i$  with  $L_G = L_H = 3$  paths and element/antenna spacing  $d = \frac{\lambda}{2}$ .

For the BAS, we consider  $L_1 = 9, 16, 25, 36, 64, 100, 225,$  and  $400$ .

For FIC, the results for different values of  $T$  are obtained by varying the total number of iterations  $I$ . As expected, a higher number of iterations yields a lower achievable rate loss, at the cost of a higher channel estimation overhead, and we note that within  $10^3$  estimations the achievable rate loss is less than 10%. We also note that, for a higher value of  $L_i$ , a lower  $\epsilon$  is typically obtained. Moreover, changing the number of explored RIS configurations across the iterations yields a further performance improvement. Lastly, when comparing Figs. 3 and 4, we note that when more paths are present a longer time  $T$  is required, and the finer the grid, the higher the minimum value of the achievable rate loss: indeed, the function relating the angles at I (thus the RIS configuration)

to the achievable rate is more complex, and it is harder to find the global maximum. Furthermore, it can be seen that for many of the considered grids  $\epsilon$  tends to saturate without further reducing the achievable rate loss. This is due to the fact that the algorithm locks in a local maximum.

*Impact of the Number of Channel Estimates:* Until now we have considered a single channel estimate at each iteration of the FIC algorithm: such estimates are affected by the noise, which has also an impact on the estimate of the achievable rate and thus the evolution of the RIS configuration search in the FIC algorithm. Performing  $K > 1$  channel estimates and then averaging the estimates before computing the achievable rate would provide a better result, at the cost of a longer estimation time, since, still assuming a unitary time for a single estimate, we have  $T_0 = K$ . Fig. 5 shows  $\epsilon$  as a function of  $T$  for a number of estimates per iteration  $K = 1, 2, 3, 4,$  and  $5$ . The error floor of  $\epsilon$  is reduced as  $K$  increases, thus if low achievable rate losses are targeted it is advantageous to increase the number of channel estimates per iteration. However, whenever a value of  $\epsilon$  is reachable for multiple values of  $K$ , it is convenient to choose the minimum  $K$  to minimize the estimation time  $T$ .

*Multiple Starting Points:* We have also tested the multiple starting points approach, and Fig. 6 shows  $\epsilon$  as a function of  $T$  for  $P = 1$  and  $4$  starting points,  $L_G = L_H = 3$  paths, and  $d = \frac{\lambda}{2}$ . In particular, we consider  $L_i = 9, i = 1, \dots, I$ , and, in addition to this, for  $P = 4$  also the case  $L_1 = 64, L_{i>1} = 9$ . The  $P$  starting points provide the highest achievable rate among the  $P$  configurations tested at the first iteration. We note an advantage of the multiple starting point approach at the cost of almost four times the number of channel estimates.

*Comparison With Respect to BAS:* Fig. 7 shows the percentage reduction of  $T_{FIC}$  with respect to  $T_{BAS}$ , named  $\Delta_T \%$ , to obtain a target  $\epsilon$  for  $d = \lambda/2$  and  $L_G = L_H = 3$ . When compared to the BAS configuration, we note that FIC

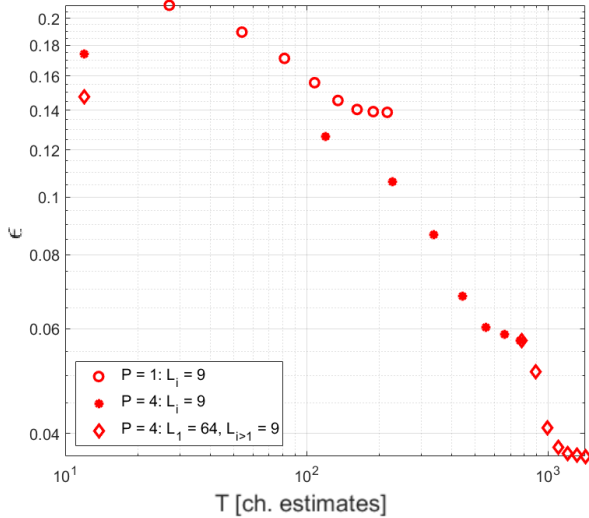


Figure 6. Average normalized achievable rate loss with  $P = 1$  and 4 starting points,  $L_i = 9$ ,  $L_G = L_H = 3$  paths, and element/antenna spacing  $d = \frac{\lambda}{2}$ .

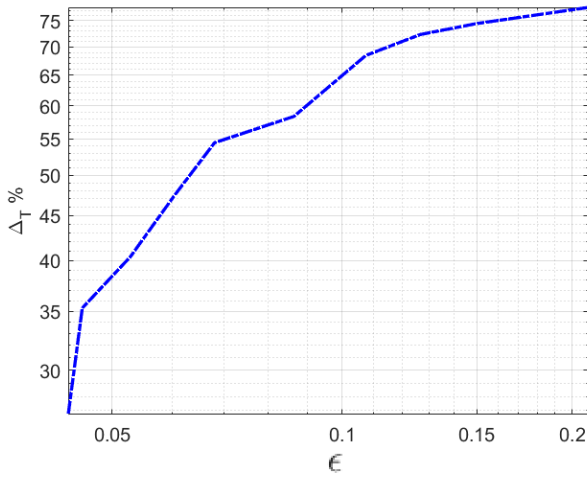


Figure 7. Percentage reduction of  $T_{FIC}$  with respect to  $T_{BAS}$  for a target  $\epsilon$ , with  $L_G = L_H = 3$  paths and element/antenna spacing  $d = \frac{\lambda}{2}$ .

significantly improves the quality of the selected configuration, with a sharp decrease in the achievable rate loss. This turns in a decrease of at least about 30% in the number of channel estimates required to reach a target  $\epsilon$ .

## V. CONCLUSIONS

In this paper, we have proposed a novel technique to find the configuration of a RIS for the uplink of a cellular system operating at mmWave frequencies. Numerical results have compared the performance of the proposed approach with a baseline solution where a fixed set of configurations is explored and the configuration providing the highest achievable rate is selected. We conclude that the proposed procedure is effective and shows a much faster convergence to a close-to-optimal configuration. We have also explored the impact

of the number of channel estimates per iteration and the multiple-starting-point approach for further optimization of the proposed scheme.

## REFERENCES

- [1] C. Huang, A. Zappone, G.C. Alexandropoulos, M. Debbah and C. Yuen, "Reconfigurable intelligent surfaces for energy efficiency in wireless communication," *IEEE Trans. Wireless Commun.*, vol. 18, pp. 4157–5409, 2019.
- [2] M. Giordani, M. Polese, A. Roy, D. Castor, and M. Zorzi, "A tutorial on beam management for 3GPP NR at mmWave frequencies," *IEEE Commun. Surveys & Tut.*, vol. 21, no. 1, pp. 173–196, Jan. 2019.
- [3] W. Attaoui, K. Bouraqia, and E. Sabir, "Initial access and beam alignment for mmWave and terahertz communications," *IEEE Access*, vol. 10, pp. 35363–35397, Oct. 2022.
- [4] M. Najafi, V. Jamali, R. Schober, and H.V. Poor, "Physics-based modeling and scalable optimization of large intelligent reflecting surface," *IEEE Trans. Commun.*, vol. 69, no. 4, pp. 2673–2691, Apr. 2021.
- [5] B. Zheng and R. Zhang, "Intelligent reflecting surface-enhanced OFDM: channel estimation and reflection optimization," *IEEE Wirel. Commun. Letters*, vol. 9, no. 4, pp. 518–522, Sept. 2020.
- [6] B. Zheng, C. You, and R. Zhang, "Intelligent reflecting assisted multi-user OFDM: channel estimation and training design," *IEEE Trans. Wirel. Commun.*, vol. 19, no. 12, pp. 8315–8329, Dec. 2020.
- [7] V. Jamali, M. Najafi R. Schober, and H.V. Poor, "Power efficiency, overhead, and complexity tradeoff of IRS codebook design-quadratic phase-shift profile," *IEEE Commun. Letters*, vol. 25, no. 6, pp. 2048–2052, June 2021.
- [8] G.C. Alexandropoulos, V. Jamali, R. Schober, and H.V. Poor, "Near-Field Hierarchical Beam Management for RIS-Enabled Millimeter Wave Multi-Antenna Systems," in Proc. *IEEE 12th SAM Signal Processing Workshop*, pp. 460–464, 2022.
- [9] M. Rahal, B. Denis, K. Keykhosravi, F. Keskin, B. Uguen, G.C. Alexandropoulos, and H. Wymeersch, "Arbitrary beam pattern approximation via RISs with measured elements responses," <https://arxiv.org/abs/2203.07225>, 2022.
- [10] M. Rahal, B. Denis, K. Keykhosravi, F. Keskin, B. Uguen, G.C. Alexandropoulos, and H. Wymeersch, "Performance of RIS-aided nearfield localization under beams approximation from real hardware characterization," <https://arxiv.org/abs/2203.15176v1>, 2023.
- [11] W.R. Ghanem, V. Jamali, M. Schellmann, H. Cao, J. Eichinger, and R. Schober, "Optimization-based phase-shift codebook design for large IRSs," <https://arxiv.org/abs/2203.01630v2>, 2022.
- [12] Z.Q. He, and X. Yuan, "Cascaded channel estimation for large intelligent metasurface assisted massive MIMO," *IEEE Wireless Commun. Lett.*, vol. 9, no. 2, pp. 210–214, Feb. 2020.
- [13] C. You, B. Zheng, and R. Zhang, "Channel estimation and passive beamforming for intelligent reflecting surface: discrete phase shift and progressive refinement," *IEEE J. Sel. Areas Commun.*, vol. 38, no. 11, pp. 2604–2620, Nov. 2020.
- [14] C. Psomas, and I. Krikidis, "Low-complexity random rotation-based schemes for intelligent reflecting surfaces," *IEEE Trans. Wireless Commun.*, vol. 20, no. 8, pp. 5212–5225, Aug. 2021.
- [15] G.C. Alexandropoulos, V. Jamali, R. Schober, and H.V. Poor, "Near-field channel estimation for RIS-enabled millimeter wave MIMO communication systems," in Proc. *IEEE SAM Signal Process Workshop*, pp. 1–5, 2022.
- [16] J. An, C. Xu, L. Gan, and L. Hanzo, "Low-complexity channel estimation and passive beamforming for RIS-assisted MIMO systems relying on discrete phase shifts," *IEEE Trans. Commun.*, vol. 70, no. 2, pp. 1245–1260, Feb. 2022.
- [17] X. Hu, C. Zhong, Y. Zhang, X. Cheng, and Z. Zhang, "Location information aided multiple intelligent reflecting surface systems," *IEEE Trans. Commun.*, vol. 68, no. 12, pp. 7948–7962, Dec. 2020.
- [18] M. Rahal, B. Denis, K. Keykhosravi, F. Keskin, B. Uguen, and H. Wymeersch, "Constrained RIS phase profile optimization and time sharing for near-field localization," in Proc. *IEEE 95th Vehicular Technology Conf. (VTC)*, pp. 1–6 2022.
- [19] S. Hur, S. Baek, B. Kim, Y. Chang, A.F. Molisch, T.D. Rappaport, K. Haneda, and J. Park, "Proposal on Millimeter-Wave channel modeling for 5G cellular system," *IEEE Journal of Selected Topics in Signal Processing*, vol. 10, no. 3, pp. 454–469, Mar. 2016.